View metadata, citation and similar papers at core.ac.uk

brought to you by CORE

provided by NASA Technical Reports Server

NASA CR-766

THE FLUTTER OF TOWED RIGID DECELERATORS

By Richard H. MacNeal

Distribution of this report is provided in the interest of information exchange. Responsibility for the contents resides in the author or organization that prepared it.

Prepared under Contract No. NAS 1-5605 by
ASTRO RESEARCH CORPORATION
Santa Barbara, Calif.

for Langley Research Center

NATIONAL AERONAUTICS AND SPACE ADMINISTRATION

For sale by the Clearinghouse for Federal Scientific and Technical Information
Springfield, Virginia 22151 – CFSTI price $3.00

CONTENTS

THE FLUTTER OF TOWED RIGID DECELERATORS

By Richard H. MacNeal
Astro Research Corporation

SUMMARY

The flutter of a rigid drag body towed behind a massive primary body by means of a flexible cable is examined. Nyquist's criterion is used to show that, in order to prevent flutter for all cable lengths, the real part of the mechanical input impedance to the drag body at the cable attachment point must be positive at all frequencies. This result is used to derive relationships between geometric and aerodynamic parameters that define the boundary for unconditional stability (stability at all cable lengths).

The most important general results are that stability is improved by moving the cable attachment point forward and that the optimum position of the center of gravity is midway between the cable attachment point and a modified center of pressure, where the modification depends primarily on C_{mq} .

The results of the general analysis are applied to a conical shell decelerator in Newtonian flow. It is shown that a conical shell towed from its apex and with uniform surface mass density is unconditionally stable provided that the semi-apex angle exceeds $15.5°$.

INTRODUCTION

A towed aerodynamic decelerator system consists of three elements, as shown in Figure 1: a drag body, a primary body or payload, and a flexible cable connecting the two bodies. Flutter of such systems has been observed in wind tunnels, so that the conditions under which flutter can exist are of interest.

The following assumptions will be made concerning the elements of a towed decelerator system.

Drag Body.— The drag body is rigid and is connected to the cable at a forward apex. It is symmetrical with respect to at least two planes and does not spin.

Primary Body.— The primary body is assumed to be so massive that all of the drag force is transmitted to it, and that its transverse motions are negligibly small. These assumptions correspond to wind tunnel conditions.

Cable.— The cable is flexible and inextensional, i.e., it transmits no bending or twisting moments and does not deform parallel to its axis. Aerodynamic forces acting on the cable are neglected. The distributed mass of the cable is not neglected.

In view of the above assumptions, the system may be considered, for purpose of analysis, as consisting of two objects, the drag body and the cable, that move in a plane and that interact with each other by virtue of the lateral translation at their point of connection. The motions of the drag body can, furthermore, be described by two quantities - rotation in the plane of motion, and lateral translation at the point of connection to the cable. Positive sign conventions for these motions are established in Figure 1.

SYMBOLS

B_{11}, B_{12}, B_{21}, B_{22} aerodynamic damping coefficients, see Equation (5)

C_D drag coefficient

C_{mq} pitching moment derivative of pitching velocity

C_{nq} normal force derivative of pitching velocity

$C_{n\alpha}$ normal force derivative of angle of attack

F external lateral force applied at cable attachment point

F_c lateral force on cable

F_d lateral force on drag body

h lateral translation at cable attachment point

I second moment of inertia about cable attachment point

$i = \sqrt{-1}$

K_c effective spring constant of cable

K_{12}, K_{22} aerodynamic stiffness coefficients, see Equation (5)

k radius of gyration in pitch about cable attachment point

k_o radius of gyration, in pitch, about center of gravity

ℓ_b height of cone

ℓ_c length of cable

ℓ_{cg} distance from cable attachment point to center of gravity

ℓ_{cp} distance from cable attachment point to center of pressure

M mass of drag body

m mass per unit length of cable

$p = \frac{d}{dt}$

R base radius of drag body

R_d real part of Z_d

S first moment of inertia about cable attachment point

T tension in cable

t time

X_c imaginary part of Z_c

X_d imaginary part of Z_d

Z_c mechanical impedance of cable, see Equation (4)

Z_d mechanical impedance of drag body, see Equation (6)

$\beta = k^2/\ell_{cg}\ell_{cp}$

γ semi-apex angle of cone

γ_c minimum semi-apex angle for unconditional stability

δ see Equation (2)

θ pitch angle in inertial space

ω frequency, rad/sec

$\lambda = RC_{nq}/\ell_{cp}C_{n\alpha}$

$\eta = R^2C_{mq}/\ell^2_{cp}C_{n\alpha}$

MATHEMATICAL REPRESENTATION OF THE CABLE

Since the mass of the flexible cable is distributed, it is not possible to accurately describe the motions of the cable by means of a finite set of coordinates. The motion of the cable at the connection point could be adequately approximated by a small number of vibration modes. However, it is more convenient, in the approach to be taken, to describe the motion at the connection point by means of the following relationship between force and displacement derived in Appendix A.

$$\frac{F_c}{h} = K_c = T\delta \cdot \mathrm{ctn}\left(\delta \ell_c\right) \tag{1}$$

where

$$\delta = \omega \sqrt{\frac{m}{T}} \tag{2}$$

and

T = tension in cable

m = mass per unit length of the cable

ℓ_c = length of the cable

ω = frequency, rad/sec

Note that, for $\omega = 0$, $K_c = T/\ell_c$ in agreement with elementary theory, and that as the frequency increases, the stiffness coefficient repeatedly spans the entire range of values from $-\infty$ to $+\infty$. In subsequent work, use will be made of the mechanical impedance of the cable at real frequencies

$$Z_c \equiv \frac{F_c}{\frac{dh}{dt}} = \frac{K_c}{i\omega} = -i\sqrt{mT}\cdot\mathrm{ctn}\left(\omega\ell_c\sqrt{\frac{m}{T}}\right) \tag{3}$$

In terms of the differential operator $p = i\omega$,

$$Z_c = -\sqrt{mT}\cdot\mathrm{ctnh}\left(p\ell_c\sqrt{\frac{m}{T}}\right) \tag{4}$$

MATHEMATICAL REPRESENTATION OF THE DRAG BODY

The relationship between forces and motions of the drag body is represented by the following matrix equation.

$$\begin{bmatrix} B_{11}p + Mp^2 & K_{12} - B_{12}p - Sp^2 \\ -B_{21}p - Sp^2 & K_{22} + B_{22}p + Ip^2 \end{bmatrix} \begin{Bmatrix} h \\ \theta \end{Bmatrix} = \begin{Bmatrix} F_d \\ 0 \end{Bmatrix} \tag{5}$$

The coefficients B_{11}, B_{12}, B_{21}, B_{22}, K_{12} and K_{22} are due to aerodynamic forces. The relationship between these coefficients and the aerodynamic derivatives for the drag body is presented in Appendix B. The sign convention for motions (see Fig. 1) is such that all coefficients appearing in Equation (5) are positive if:

(1) The center of gravity is aft of the connection point to the cable.

(2) The center of pressure is aft of the connection point.

(3) Positive angle of attack produces negative lift. Note that this accounts for the positive sign of K_{12}. It is the normal condition for blunt drag bodies, but not for lifting bodies.

(4) Damping in pitch, C_{mq}, is stabilizing.

(5) The normal force derivative of pitching velocity, C_{nq}, is either positive or not too large a negative number.

The mechanical impedance of the drag body, as viewed from the connection point to the cable, is from Equation (5):

$$Z_d = \frac{F_d}{\dot{h}} = \frac{F_d}{ph} = B_{11} + Mp - \frac{\left(-K_{12} + B_{12}p + Sp^2\right)\left(B_{21}p + Sp^2\right)}{\left(K_{22} + B_{22}p + Ip^2\right)p} \qquad (6)$$

GENERAL THEORY

The stability of the decelerator system can be examined by considering the relationship between lateral translation at the connection point, and an external force applied to that point,

$$F = F_c + F_d = \left(Z_c + Z_d\right)\dot{h} \qquad (7)$$

where Z_c is the mechanical impedance of the cable and Z_d is the mechanical impedance of the drag body. For self-excited motions the external force, F, is zero.

In general the coefficient $Z_c + Z_d$ is a function of the differential operator $p = d/dt$.

In the present instance Z_d is a ratio of two polynomials given by Equation (6), and Z_c is a transcendental function

given by Equation (4). It is shown in Laplace transform theory that the system is stable provided that $Z_c + Z_d$ has no roots with positive real parts, i.e. provided that the zeroes of $Z_c + Z_d$ occur in the left half of the p plane.

The function $Z_c + Z_d$ also has poles. The poles correspond to eigenvalues of the system when it is rigidly restrained at the connection point such that $\dot{h} = 0$ in Equation (7) for any value of the constraining force, F.

The significance of the zeroes and poles of $Z_c + Z_d$ results from Nyquist's theorem (Reference 1), which is: —— Consider the function $Z(p)$ which is regular except at isolated poles. Then, if the function $Z(p)$ is plotted as p assumes values along the imaginary axis from $-\infty$ to $+\infty$, the number of times that the plot encircles the origin is equal to the difference between the number of zeroes and poles in the right half of the p plane. ——

Hence, if it can be shown, on general grounds, that $Z_c + Z_d$ has no poles in the right half plane, then the system will be stable if the Nyquist plot of $Z_c + Z_d$ does not encircle the origin. The condition for the absence of poles in the right half plane is easily demonstrated in the present instance since, as observed above, the poles of $Z_c + Z_d$ are the eigenvalues of the system when rigidly restrained at the cable connection point. If the system is stable when so constrained, there will be no poles in the right half of the p plane.

A rigid constraint removes the coupling between the drag body and the cable. The cable will be stable in this condition because, by assumption, no aerodynamic forces —— destabilizing or otherwise —— act on it. We can, if we like, assume the existence of a small amount of structural damping in the cable to shift its zeroes and poles slightly to the left of the imaginary axis. The drag body is stable when h is constrained to zero provided that K_{22}, B_{22} and I in Equation (5) are all positive. This condition is assumed. Thus the constrained system is stable, $Z_c + Z_d$ has no poles in the right half plane, and the towed decelerator will be stable provided that the plot of $Z_c + Z_d$ as a function of frequency, does not encircle the

origin as ω varies from $-\infty$ to $+\infty$.

It is apparent, from Equation (3) that Z_c is restricted to the imaginary axis for $p = i\omega$ and that it repeatedly spans the entire axis as frequency is varied. We will later require more exact knowledge of Z_d, but for the present, let it be assumed that the plot of Z_d as a function of frequency has the character shown in Figure 2.

The plot of Z_d for $\omega < 0$ is the mirror image about the real axis of the plot for $\omega > 0$. The important property of Z_d shown in Figure 2, is that its real part is negative for $\omega_1 < \omega < \omega_2$. While ω is in this range, let it be assumed that the plot of Z_c moves upward along the imaginary axis from X_{c1} to X_{c2}. That Z_c always moves upward is apparent from Equation (3).

Now if Z_c is added to Z_d, it is apparent that the plot of $Z_c + Z_d$ will encircle the origin if $X_{d1} + X_{c1} < 0$ and $X_{d_2} + X_{c_2} > 0$. If this is true, then the imaginary part of $Z_c + Z_d$, namely $X_c + X_d$, must be zero at some point in the interval $\omega_1 < \omega < \omega_2$. Examination of Figure 2 yields the following theorems.

If Z_d has the character shown in Figure 2: -

(1) The system will be unstable if, and only if, the imaginary part of $Z_c + Z_d$ vanishes at some point in the frequency interval within which the real part of Z_d is negative.

(2) If the zeroes of the imaginary part of $Z_c + Z_d$ for $p - i\omega$ are examined, the system will be stable if, and only if, the real part of Z_d is positive at all the zeroes.

(3) If the real part of Z_d is always positive for $p = i\omega$, the system will be stable.

We are now prepared to examine the question of stability as the cable is payed out, i.e., as the length of the cable increases from zero to some large value. During this process, the value of Z_c at a given frequency, ω_o, will, from Equation (3), assume all values from $-i\infty$ to $+i\infty$. Therefore, it is inevitable that, if the real part of Z_d is negative in any small frequency range, a length of cable can be found for which the imaginary part of $Z_c + Z_d$ vanishes within the range. The system will therefore be unstable for certain ranges of cable length as long as the real part of Z_d is negative in any part of the frequency spectrum. The only way to ensure stability during cable reel-out is to insist that the real part of Z_d be positive at all frequencies. If, on the other hand, it is only required that the system be stable in its fully deployed position, the requirement on Z_d is less restrictive. Theorems (1) or (2) above may then be used to answer the stability question.

The conclusions reached above have been partially verified by wind tunnel tests. In such tests it is frequently observed that the towed decelerator passes through alternating regions of stability and instability as the length of cable is increased.

It should not be surprising that the requirement that Z_d have positive real part at all frequencies is <u>sufficient</u> for stability. This requirement merely states that the decelerator must absorb power, rather than generate power, when excited by a lateral force at the attachment point. What is perhaps less obvious is that the same requirement is <u>necessary</u> for stability at all cable lengths.

In the remainder of this paper, the conservative requirement that the real part of Z_d be positive at all frequencies will be examined. This requirement will be termed "unconditional stability", i.e., stability for all values of cable length. It is also a realistic requirement for decelerators that may be used with a variety of cables.

REQUIREMENT FOR UNCONDITIONAL STABILITY

The first task is to compute the real part of $Z_c = R_d + iX_d$ from Equation (6) with $p = i\omega$.

$$R_d = B_{11} - R.P. \left\{ \frac{\left(-K_{12} - S\omega^2 + i\omega B_{12}\right)\cdot\left(-S\omega^2 + i\omega B_{21}\right)\cdot\left(K_{22} - I\omega^2 - i\omega B_{22}\right)}{i\omega\left[\left(K_{22} - I\omega^2\right)^2 + \omega^2 B_{22}^2\right]} \right\} \quad (8)$$

In order to simplify calculation, it will be assumed that the damping coefficients, B's , are small compared to the mass and stiffness terms. This is equivalent to assuming that the mass of the drag body is large compared to the mass of the fluid it displaces. This condition is usually satisfied in supersonic flight. Eliminating second and higher power of the B's , Equation (8) becomes

$$R_d = \frac{1}{\left(K_{22} - I\omega^2\right)^2} \left\{ \begin{array}{l} B_{11}\left(K_{22} - I\omega^2\right)^2 + B_{12}\left(S\omega^2\right)\cdot\left(K_{22} - I\omega^2\right) \\ + B_{21}\left(K_{12} + S\omega^2\right)\cdot\left(K_{22} - I\omega^2\right) \\ + B_{22}\left(K_{12} + S\omega^2\right) S\omega^2 \end{array} \right\} \quad (9)$$

The decelerator system has unconditional stability only if R_d is positive. Using the limiting condition, $R_d = 0$, to express the flutter boundary, the following quadratic equation in ω^2 is obtained

$$A\omega^4 + B\omega^2 + C = 0 \quad (10)$$

where

$$\left.\begin{aligned} A &= B_{11} I^2 + B_{22} S^2 - \left(B_{12} + B_{21}\right) SI \\ B &= -2B_{11} K_{22} I + B_{12} SK_{22} + B_{21}\left(SK_{22} - IK_{12}\right) + B_{22} SK_{12} \\ C &= B_{11} K_{22}^2 + B_{21} K_{12} K_{22} \end{aligned}\right\} \qquad (11)$$

In order for a flutter boundary to exist, Equation (10) must have at least one positive real root.

Positive real roots will not occur and R_d will be positive at all frequencies if $A > 0$, $C > 0$ and $B + 2\sqrt{AC} > 0$. With some rearrangement of Equation (11) these conditions are, assuming B_{11} and K_{22} to be inherently positive

$$1 + \frac{B_{22}}{B_{11}}\left(\frac{S}{I}\right)^2 - \left(\frac{B_{12} + B_{21}}{B_{11}}\right)\frac{S}{I} > 0 \qquad (12)$$

$$1 + \frac{B_{21}}{B_{11}} \cdot \frac{K_{12}}{K_{22}} > 0 \qquad (13)$$

and

$$-2 + \left(\frac{B_{12} + B_{21}}{B_{11}}\right)\frac{S}{I} + \frac{K_{12}}{K_{22}}\left(\frac{B_{22}}{B_{11}} \cdot \frac{S}{I} - \frac{B_{21}}{B_{11}}\right)$$

$$+ 2\left[1 + \frac{B_{22}}{B_{11}}\left(\frac{S}{I}\right)^2 - \left(\frac{B_{12} + B_{21}}{B_{11}}\right)\frac{S}{I}\right]^{\frac{1}{2}} \cdot \left[1 + \frac{B_{21}}{B_{11}} \cdot \frac{K_{12}}{K_{22}}\right]^{\frac{1}{2}} > 0 \qquad (14)$$

The time has now come to convert the generalized coefficients in these equations into coefficients involving the physical properties of the drag body. Since S is the first moment of mass

about the cable attachment point, and I is the second moment, it follows that

$$\frac{S}{I} = \frac{\ell_{cg}}{k^2} \tag{15}$$

where ℓ_{cg} is the distance from the cable attachment point to the center of gravity and k is the radius of gyration about the attachment point. The ratios of aerodynamic coefficients obtained from Appendix B are:

$$\frac{K_{12}}{K_{22}} = \frac{1}{\ell_{cp}}\left(\frac{C_D}{C_{n\alpha}} - 1\right) \tag{16}$$

$$\frac{B_{22}}{B_{11}} = \ell_{cp}^2 + \frac{R\ell_{cp}C_{nq}}{C_{n\alpha}} - \frac{R^2C_{mq}}{C_{n\alpha}} \tag{17}$$

$$\frac{B_{12}}{B_{11}} = \ell_{cp} + \frac{RC_{nq}}{C_{n\alpha}} \tag{18}$$

$$\frac{B_{21}}{B_{11}} = \ell_{cp} \tag{19}$$

where

R = base radius of drag body

ℓ_{cp} = distance from cable attachment point to the center of pressure, defined as the point about which the static aerodynamic moment is zero

C_D = drag coefficient

$C_{n\alpha}$, C_{nq} = coefficient of force normal to the axis of the displaced body due, respectively, to: angle of attack, and pitching velocity.

C_{mq} = coefficient of moment due to pitching velocity

It is convenient to define the following parameters:

$$\left.\begin{aligned} \beta &= \frac{k^2}{\ell_{cg}\ell_{cp}} \\ \lambda &= \frac{RC_{nq}}{\ell_{cp}C_{n\alpha}} \\ \eta &= \frac{R^2C_{mq}}{\ell_{cp}^2C_{n\alpha}} \end{aligned}\right\} \qquad (20)$$

Substituting the above results into Equations (12), (13), and (14), the requirements for unconditional stability become

$$1 + \frac{1}{\beta^2}\left(1 + \lambda - \eta\right) - \left(2 + \lambda\right)\frac{1}{\beta} > 0 \qquad (21)$$

$$\frac{C_D}{C_{n\alpha}} > 0 \qquad (22)$$

and

$$-2 + (2 + \lambda)\frac{1}{\beta} + \left(\frac{C_D}{C_{n\alpha}} - 1\right)\cdot\left(\frac{1}{\beta}(1 + \lambda - \eta) - 1\right)$$

$$+ 2\left(\frac{C_D}{C_{n\alpha}}\right)^{\frac{1}{2}}\cdot\left(1 + \frac{1}{\beta^2}(1 + \lambda - \eta) - (2 + \lambda)\frac{1}{\beta}\right)^{\frac{1}{2}} > 0 \qquad (23)$$

It will be noted immediately that Equation (22) is always satisfied for any reasonable aerodynamic body.

Numerical values of the derivatives due to pitching velocity,

C_{nq} and C_{mq}, are not easily obtained from wind tunnel measurements. They can be estimated theoretically using, for example, Newtonian flow theory in hypersonic flow. The most that can be said without further investigation is that C_{nq} is probably small, and that C_{mq} is probably negative.

If C_{nq} and hence λ is omitted, Equation (21) becomes, upon multiplication by β^2,

$$(1 - \beta)^2 - \eta > 0 \tag{24}$$

and Equation (23) becomes, upon multiplication by β, assumed positive,

$$\left(\frac{C_D}{C_{n\alpha}} + 1\right)\cdot(1 - \beta) - \left(\frac{C_D}{C_{n\alpha}} - 1\right)\eta + 2\left(\frac{C_D}{C_{n\alpha}}\right)^{\frac{1}{2}}\cdot\left[(1 - \beta)^2 - \eta\right]^{\frac{1}{2}} > 0 \tag{25}$$

The flutter boundary is obtained by converting Equations (24) and (25) into equalities. When this is done Equation (25) may be solved for β, giving

$$\beta = 1 + \frac{\left(1 + \frac{C_D}{C_{n\alpha}}\right)\eta \pm 2\left(\frac{C_D}{C_{n\alpha}}\right)^{\frac{1}{2}}\cdot(\eta^2 - \eta)^{\frac{1}{2}}}{1 - C_{D/C_{n\alpha}}} \tag{26}$$

The (+) sign is to be used for $\frac{C_D}{C_{n\alpha}} < 1$ and the (-) sign is to be used for $\frac{C_D}{C_{n\alpha}} > 1$.

Flutter boundaries are plotted in Figure 3.

Equation (24) provides a flutter boundary only for $C_{mq} > 0$. Equation (26) provides a flutter boundary only for $C_{mq} < 0$. The latter statement is true because β as obtained from Equation (26)

is complex for $0 < \eta < 1$ and because, if $\eta > 1$, B_{22} becomes negative violating a basic assumption on which the analysis is based, see page 9. Since normally $C_{mq} < 0$, Equation (26) is the more important flutter boundary.

The following asymptotic behaviour of Equation (26) is noted:

If

$$\frac{C_D}{C_{n\alpha}} \longrightarrow 1 \qquad \beta \longrightarrow \infty \tag{27}$$

$$\frac{C_D}{C_{n\alpha}} \longrightarrow 0 \qquad \beta \longrightarrow 1 + \eta \tag{28}$$

$$\frac{C_D}{C_{n\alpha}} \longrightarrow \infty \qquad \beta \longrightarrow 1 - \eta \tag{29}$$

$$\eta \longrightarrow 0 \qquad \beta \longrightarrow 1 \tag{30}$$

$$\eta \longrightarrow 0 \qquad \frac{d\beta}{d\eta} \longrightarrow -\infty \tag{31}$$

The parameter β is directly related to the inertia properties of the drag body and hence may be used to determine flutter free balance conditions. The larger the value of β, the less severe the balance requirement. It is clear from the asymptotic behaviour of β that a drag body for which the normal force coefficient is approximately equal to the drag coefficient is inherently more stable than other configurations, provided that C_{mq} is negative.

A useful expression for the location of the center of gravity may be derived by noting that

$$k^2 = \ell_{cg}^2 + k_o^2 \tag{32}$$

where k_o is the radius of gyration about the center of gravity. Thus, employing the definition of β from Equation (20) there results

$$\ell_{cg}^2 + k_o^2 - \beta \ell_{cp} \cdot \ell_{cg} = 0 \tag{33}$$

The permissible range of ℓ_{cg} for $C_{mq} < 0$, obtained by solving Equation (33), is

$$\frac{\beta \ell_{cp}}{2} - \sqrt{\left(\frac{\beta \ell_{cp}}{2}\right)^2 - k_o^2} < \ell_{cg} < \frac{\beta \ell_{cp}}{2} + \sqrt{\left(\frac{\beta \ell_{cp}}{2}\right)^2 - k_o^2} \tag{34}$$

where β is determined from the aerodynamic requirements, Equations (21) and (23), or in case $C_{nq} = 0$, from Figure 3. Since β and ℓ_{cp} appear in product form, the product $\beta \ell_{cp}$ will, for convenience, be termed the distance from the attachment point to a "modified" center of pressure.

The following conclusions can then be drawn:

(1) Absence of flutter cannot be guaranteed unless $\beta \ell_{cp} > 2k_o$ i.e., unless the distance from the attachment point to the modified center of pressure is greater than twice the radius of gyration in pitch.

(2) The optimum position for the center of gravity is half way between the cable attachment point and the modified center of pressure.

(3) The most effective mechanical means for preventing flutter is to move the cable attachment point as far forward as possible. This can be done by attaching a relatively rigid sting to the apex of the decelerator.

The relationship described by Equation (34) is plotted in Figure 4.

FLUTTER OF A TOWED CONE IN NEWTONIAN FLOW

Consider the conical decelerator shown in Figure 5. The aerodynamic parameters of a cone in Newtonian flow are derived in Appendix C, where it is shown that

$$\ell_{cp} = \frac{2}{3} \cdot R/\sin\gamma \cdot \cos\gamma$$

$$C_{n\alpha} = 2 \cdot \cos^2 \gamma$$

$$C_D = 2 \cdot \sin^2 \gamma \qquad (35)$$

$$C_{nq} = 0$$

$$C_{mq} = \frac{-1}{9 \cdot \sin^2 \gamma}$$

where R is the base radius and γ is the semi-apex angle. Since the height of the cone $\ell_b = R/\tan\gamma$, the ratio of center of pressure to height is

$$\frac{\ell_{cp}}{\ell_b} = \frac{2}{3 \cdot \cos^2 \gamma} \qquad (36)$$

Thus for large cone angles the center of pressure is well aft of the base.

Since $C_{nq} = 0$ and $C_{mq} < 0$, Equation (26) may be used directly to obtain the flutter boundary. From the results stated in Equation (35), the aerodynamic parameters required in Equation (26) are

$$\left.\begin{aligned} \frac{C_D}{C_{n\alpha}} &= \tan^2\gamma \\ \eta = \left(\frac{R}{\ell_{cp}}\right)^2 \cdot \frac{C_{mq}}{C_{n\alpha}} &= \left(\frac{9}{4}\cdot\sin^2\gamma\cdot\cos^2\gamma\right)\cdot\left(\frac{-1}{18\cdot\sin^2\gamma\cdot\cos^2\gamma}\right) = -\frac{1}{8} \end{aligned}\right\} \quad (37)$$

Hence, by inspection of Figure 3, the largest permissible value of β varies from .875 (for $\gamma = 0$), to ∞ (for $\gamma = 45°$), and back to 1.125 (for $\gamma = 90°$). The exact functional relationship, obtained by substituting from Equation (37) into Equation (26), is

$$\beta = 1 - \frac{1 \pm 3\cdot\sin 2\gamma}{8\cdot\cos 2\gamma} \quad (38)$$

The (+) sign is used for $\gamma > 45°$ and the (-) sign is used for $\gamma < 45°$.

If the mass of the cone is uniformly distributed in a thin layer over its surface, the distance from the apex to the center of gravity is

$$\ell_{cg} = \frac{2}{3}\cdot\ell_b$$

while the square of the radius of gyration about the apex is

$$k^2 = \frac{1}{2}\cdot\ell_b^2\left(1 + \frac{1}{2}\cdot\tan^2\gamma\right)$$

Hence, using these relationships and Equation (36)

$$\beta = \frac{k^2}{\ell_{cp}\ell_{cg}} = \frac{9}{8}\cdot\cos^2\gamma\left(1 + \frac{1}{2}\cdot\tan^2\gamma\right) = \frac{9}{8}\left(1 - \frac{1}{2}\cdot\sin^2\gamma\right) \quad (39)$$

Comparing Equations (38) and (39), it is seen that the cone will flutter at some cable length for small semi-apex angles, and that it is unconditionally stable for large semi-apex angles. The smallest value of γ for which the towed conical shell is

unconditionally stable, as obtained by equating β in Equations (38) and (39), is $\gamma_c = 15.5°$.

The result that towed cones with large semi-apex angles are unconditionally stable contradicts available experimental results. Tests in the Mach Number range from 1.57 to 4.65 reported in Reference 2 indicate that cones with 30°, 35° and 40° semi-apex angles are stable but that a cone with a 45° semi-apex angle is unstable. Instability appeared to be associated with shock wave detachment.

Some insight into the stability problem for towed cones may be obtained from examination of Figure 6 where the location of the center of pressure predicted by Equation (36) is compared with the location required for stability, as obtained from Equation (38) and the formulas for ℓ_{cg} and k^2 . It will be observed that stability at semi-apex angles greater than 45° requires a rapid rearward shift of the center of pressure. Newtonian impact theory predicts such a shift, whereas available experimental evidence suggests that it does not occur for Mach numbers below 5.

Flared cones also have a tendency toward instability. Supersonic measurements on flared cones with tension shell geometry (Ref. 3), indicate that the center of pressure is located approximately ½ base radius forward of the base regardless of cone height, and that the ratio of the drag coefficient to the normal force coefficient is approximately equal to 5, both of which are unfaborable characteristics for flutter. It has been observed that the stability of a flared cone can be improved by moving the cable attachment point forward and also by shifting the center of gravity forward, as predicted by the results contained in this report.

An important conclusion of the present study is that experimental measurements of center of pressure and normal force coefficient will be required in order to permit prediction of the flutter characteristics of towed supersonic decelerators.

Astro Research Corporation
Santa Barbara, California, September 30, 1966.

APPENDIX A

EFFECTIVE SPRING CONSTANT OF THE CABLE

The differential equation for the cable is

$$m \cdot \frac{\partial^2 h}{\partial t^2} - T \cdot \frac{\partial^2 h}{\partial x^2} = 0 \qquad \text{(A-1)}$$

with the boundary conditions

$$h = 0 \quad \text{at} \quad x = 0$$

$$F_c = T \cdot \frac{dh}{dx} \quad \text{at} \quad x = \ell_c$$

where

h = lateral translation of cable

m = mass per unit length

T = tension

F_c = force applied to cable at free end

ℓ_c = length of cable

A general solution that satisfies the differential equation and the boundary condition at $x = 0$ is

$$h = e^{i\omega t} \cdot \sin(\delta x) \qquad \text{(A-2)}$$

where

$$\delta = \omega \sqrt{\frac{m}{T}} \qquad \text{(A-3)}$$

The relationship between force and displacement at the free end is

$$K_c = \frac{F_c}{h} = \frac{T \cdot \frac{dh}{dx}}{h} = T\delta \cdot \mathrm{ctn}\left(\delta \ell_c\right) \qquad \text{(A-4)}$$

APPENDIX B.

AERODYNAMIC COEFFICIENTS

The aerodynamic forces acting on a drag body are shown in Figure B-1. The center of pressure is defined as the point about which there is no steady moment due to angle of attack.

For small motion the aerodynamic forces and moment about the center of pressure in the pitch plane may be approximated by

$$F_n = qA_B\left[C_{n\alpha}\cdot\alpha + C_{nq}\cdot\frac{R}{V}\cdot\dot{\theta} + C_{n\dot{\alpha}}\cdot\frac{R}{V}\cdot\dot{\alpha}\right] \qquad \text{(B-1)}$$

$$F_a = qA_B\left[C_D + C_{a\alpha}\alpha + C_{aq}\cdot\frac{R}{V}\cdot\dot{\theta} + C_{a\dot{\alpha}}\cdot\frac{R}{V}\cdot\dot{\alpha}\right] \qquad \text{(B-2)}$$

$$M = qA_BR\left[C_{mq}\cdot\frac{R}{V}\cdot\dot{\theta} + C_{m\dot{\alpha}}\cdot\frac{R}{V}\cdot\dot{\alpha}\right] \qquad \text{(B-3)}$$

where the C's are dimensionless coefficients and

q = dynamic pressure $\left(= \frac{1}{2}\cdot\rho V^2\right)$

A_B = base area $\left(= \pi R^2\right)$

The drag coefficient, C_D, rather than the axial force coefficient, C_a, is used in Equation (B-2), because the two coefficients are identical at zero angle of attack and because C_D is a more familiar term.

The angle of attack measured to the relative wind velocity is related to motion of the drag body by

$$\alpha = \theta - \frac{\dot{h}_{cp}}{V} \qquad \text{(B-4)}$$

When α is substituted into the aerodynamic force equations, it is permissible to omit the terms proportional to $\ddot{h}_{cp}$. These

terms represent an apparent mass which will be neglible in most practical cases. The result is

$$F_n = qA_B\left[C_{n\alpha}\left(\theta - \frac{\dot{h}_{cp}}{V}\right) + \frac{R}{V}\left(C_{nq} + C_{n\dot{\alpha}}\right)\dot{\theta}\right] \qquad \text{(B-5)}$$

$$F_a = qA_B\left[C_D + C_{a\alpha}\left(\theta - \frac{\dot{h}_{cp}}{V}\right) + \frac{R}{V}\left(C_{aq} + C_{a\dot{\alpha}}\right)\dot{\theta}\right] \qquad \text{(B-6)}$$

$$M = qA_B\left[\frac{R^2}{V}\left(C_{mq} + C_{m\dot{\alpha}}\right)\dot{\theta}\right] \qquad \text{(B-7)}$$

The coefficients $C_{n\dot{\alpha}}$, $C_{a\dot{\alpha}}$, and $C_{m\dot{\alpha}}$ will be omitted for conciseness. Their addition to the derivatives of pitching velocity is implied.

In the flutter analysis the lateral force and the moment about the cable attachment point are required expressed in terms of the pitch angle and the lateral translation at the attachment point. For this purpose, calculate

$$F_h = F_n \cdot \cos\theta - F_a \cdot \sin\theta \qquad \text{(B-8)}$$

$$M_c = M - \ell_{cp} F_n \qquad \text{(B-9)}$$

and substitute

$$h_{cp} = h - \ell_{cp}\theta \qquad \text{(B-10)}$$

Since we are only concerned with small motions, we may set $\cos\theta = 1$ and $\sin\theta = \theta$ in (B-8) and retain only terms

proportional to the first power of the displacements. The results are

$$F_h = qA_B\left[\left(C_{n\alpha} - C_D\right)\theta - C_{n\alpha}\cdot\frac{\dot{h}}{V} + \left(\ell_{cp}C_{n\alpha} + RC_{nq}\right)\frac{\dot{\theta}}{V}\right] \qquad \text{(B-11)}$$

$$M_c = qA_B\left[-\ell_{cp}C_{n\alpha}\theta + \ell_{cp}C_{n\alpha}\cdot\frac{\dot{h}}{V} + \left(C_{mq}R^2 - \ell_{cp}RC_{nq} - \ell_{cp}^2C_{n\alpha}\right)\frac{\dot{\theta}}{V}\right] \qquad \text{(B-12)}$$

Referring to Equation (5) of the main text, it is seen that

$$K_{12} = qA_B\left(C_D - C_{n\alpha}\right)$$

$$K_{22} = qA_B\ell_{cp}C_{n\alpha}$$

$$B_{11} = \frac{qA_B}{V}\cdot C_{n\alpha}$$

$$B_{12} = \frac{qA_B}{V}\left(\ell_{cp}C_{n\alpha} + RC_{nq}\right)$$

$$B_{21} = \frac{qA_B}{V}\left(\ell_{cp}C_{n\alpha}\right)$$

$$B_{22} = \frac{qA_B}{V}\left(\ell_{cp}^2C_{n\alpha} + \ell_{cp}RC_{nq} - R^2C_{mq}\right)$$

APPENDIX C.

AERODYNAMIC FORCES ON A CONE IN NEWTONIAN FLOW

The aerodynamic pressure on a surface in Newtonian flow is given by

$$p = \rho V_n^2 \tag{C-1}$$

where ρ is the density and V_n is the component of flow normal to the surface in the free stream.

Consider the cone shown in Figure C-1. The wind direction lies in the X , Z plane with angle of attack α_c with respect to the axis of the cone at its apex. The X and Z components of relative velocity for small values of α_c and the pitching velocity, $\dot{\theta}$, are

$$V_x = V - Z\dot{\theta} \tag{C-2}$$

$$V_z = V\alpha_c + X\dot{\theta} \tag{C-3}$$

where X and Z are measured from the apex.

The direction cosines of the inward normal to the surface in the X and Z directions are

$$a_x = \sin\gamma \tag{C-4}$$

$$a_z = -\cos\gamma \cdot \cos\varphi \tag{C-5}$$

The component of velocity normal to the surface is

$$V_n = a_x V_x + a_z V_z = \sin\gamma\cdot(V - Z\dot{\theta}) - \cos\gamma\cdot\cos\varphi\cdot(V\alpha_c + X\dot{\theta}) \qquad (C\text{-}6)$$

Substituting $Z = X\cdot\tan\gamma\cdot\cos\varphi$, the square of the normal component of velocity is

$$\left.\begin{aligned} V_n^2 = {} & \sin^2\gamma(V - X\cdot\tan\gamma\cdot\cos\varphi\dot{\theta})^2 + \cos^2\gamma\cdot\cos^2\varphi\cdot(V\alpha_c + X\dot{\theta})^2 \\ & - 2\cdot\sin\gamma\cdot\cos\gamma\cdot\cos\varphi\cdot(V - X\cdot\tan\gamma\cdot\cos\varphi\dot{\theta})\cdot(V\alpha_c + X\dot{\theta}) \end{aligned}\right\} (C\text{-}7)$$

Retaining only terms to first order in α and $\dot{\theta}$, and substituting into (C-1), the pressure is

$$p = \rho V^2\left[\sin^2\gamma - 2\cdot\sin\gamma\cdot\cos\varphi\left(\cos\gamma\cdot\alpha_c + \frac{X\dot{\theta}}{V\cdot\cos\gamma}\right)\right] \qquad (C\text{-}8)$$

The axial and lateral force resultants are obtained from

$$F_a = \int a_x p\,dA \qquad (C\text{-}9)$$

$$F_n = \int a_z p\,dA \qquad (C\text{-}10)$$

The pitching moment about the apex is obtained from

$$M_c = \int\left(a_x Z - a_z X\right)p\,dA \qquad (C\text{-}11)$$

The element of area is

$$dA = \frac{\tan\gamma}{\cos\gamma}\cdot x\,dx\,d\varphi \qquad (C\text{-}12)$$

Substituting for the factors appearing in Equations (C-9), (C-10), and (C-11), and carrying out the integration, we obtain

$$F_a = qA_B 2 \cdot \sin^2\gamma \quad \text{(to zero order in } \alpha_c \text{ and } \dot{\theta}) \tag{C-13}$$

and

$$F_n = qA_B\left[2 \cdot \cos^2\gamma \cdot \alpha_c + \frac{4}{3} \cdot \frac{R\dot{\theta}}{V \cdot \tan\gamma}\right] \tag{C-14}$$

$$M_c = -qA_B\left[\frac{4R}{3 \cdot \tan\gamma} \cdot \alpha_c + \frac{R^2\dot{\theta}}{V \cdot \sin^2\gamma}\right] \tag{C-15}$$

where

$q = \frac{1}{2} \cdot \rho V^2$ = dynamic pressure

$A_B = \pi R^2$ = base area

R = base radius

The above results may be put into standard form by a transformation to the center of pressure.

The location of the center of pressure is obtained from

$$M_{cp}(\alpha) = M_c(\alpha) + \ell_{cp} F_n(\alpha) = 0 \tag{C-16}$$

so that from (C-14) and (C-15)

$$\ell_{cp} = -\frac{M_c(\alpha)}{F_n(\alpha)} = R \cdot \frac{2}{3 \cdot \sin\gamma \cdot \cos\gamma} \tag{C-17}$$

Now the angle of attack at the apex is related to the angle of attack at the center of pressure by

$$\alpha_c = \alpha - \frac{\ell_{cp}}{V}\cdot\dot{\theta} \tag{C-18}$$

so that, substituting into (C-14)

$$F_n = qA_B\left[2\cdot\cos^2\gamma\cdot\alpha + \left(\frac{4}{3\cdot\tan\gamma} - 2\cdot\cos^2\gamma\cdot\frac{\ell_{cp}}{R}\right)\frac{R\dot{\theta}}{V}\right] \tag{C-19}$$

The coefficient of $R\dot{\theta}/V$ is zero, as may be seen by substituting for ℓ_{cp} from (C-17). The moment about the center of pressure is

$$\left.\begin{aligned} M &= M_c + \ell_{cp}F_n \\ &= qA_B\cdot\frac{\dot{\theta}}{V}\left[\frac{4R\ell_{cp}}{3\cdot\tan\gamma} - \frac{R^2}{\sin^2\gamma}\right] \\ &= qA_B\cdot\frac{R^2}{V}\left(-\frac{1}{9\cdot\sin^2\gamma}\right)\dot{\theta} \end{aligned}\right\} \tag{C-20}$$

where the value of ℓ_{cp} has been substituted from (C-17). By comparing (C-13), (C-19), and (C-20) with Equations (B-1), (B-2), and (B-3) of Appendix B, it is concluded that, for a right circular cone in Newtonian flow,

$$\left.\begin{aligned} C_D &= 2\cdot\sin^2\gamma \\ C_{n\alpha} &= 2\cdot\cos^2\gamma \\ C_{nq} &= 0 \\ C_{mq} &= \frac{-1}{9\cdot\sin^2\gamma} \end{aligned}\right\} \tag{C-21}$$

REFERENCES

1. Nyquist, H.: Regeneration Theory. Bell System Tech. J., vol. 77, Jan. 1932, pp. 126-147.

2. Charczenko, N.; and McShera, J.T.: Aerodynamic Characteristics of Towed Cones Used As Decelerators At Mach Numbers From 1.57 to 4.65. NASA TN D-994, 1961.

3. Robinson, J. C.; Jordan, A. W.: Exploratory Experimental Aerodynamic Investigation Of Tension Shell Shapes At Mach 7. NASA TN D-2994, 1965.

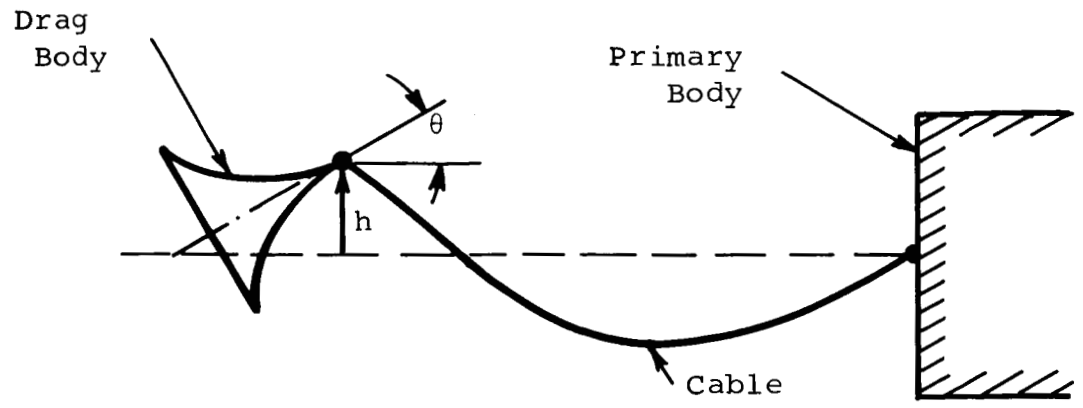

Figure 1. -- Towed Decelerator System

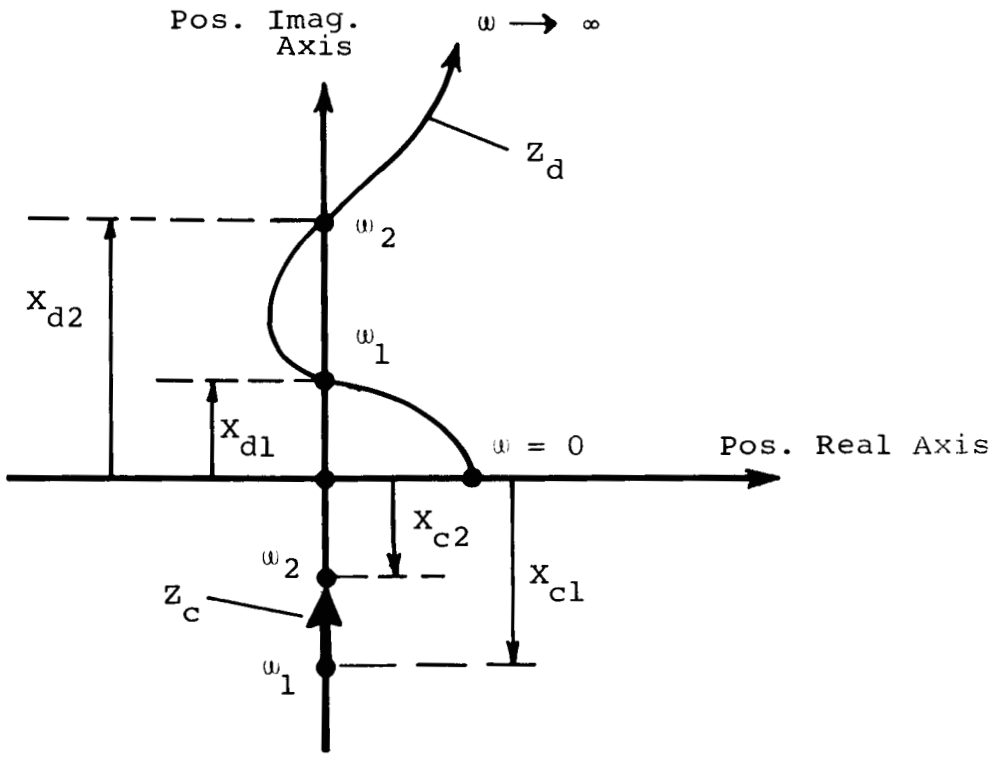

Figure 2 — Nyquist Plot of Z_c and Z_d

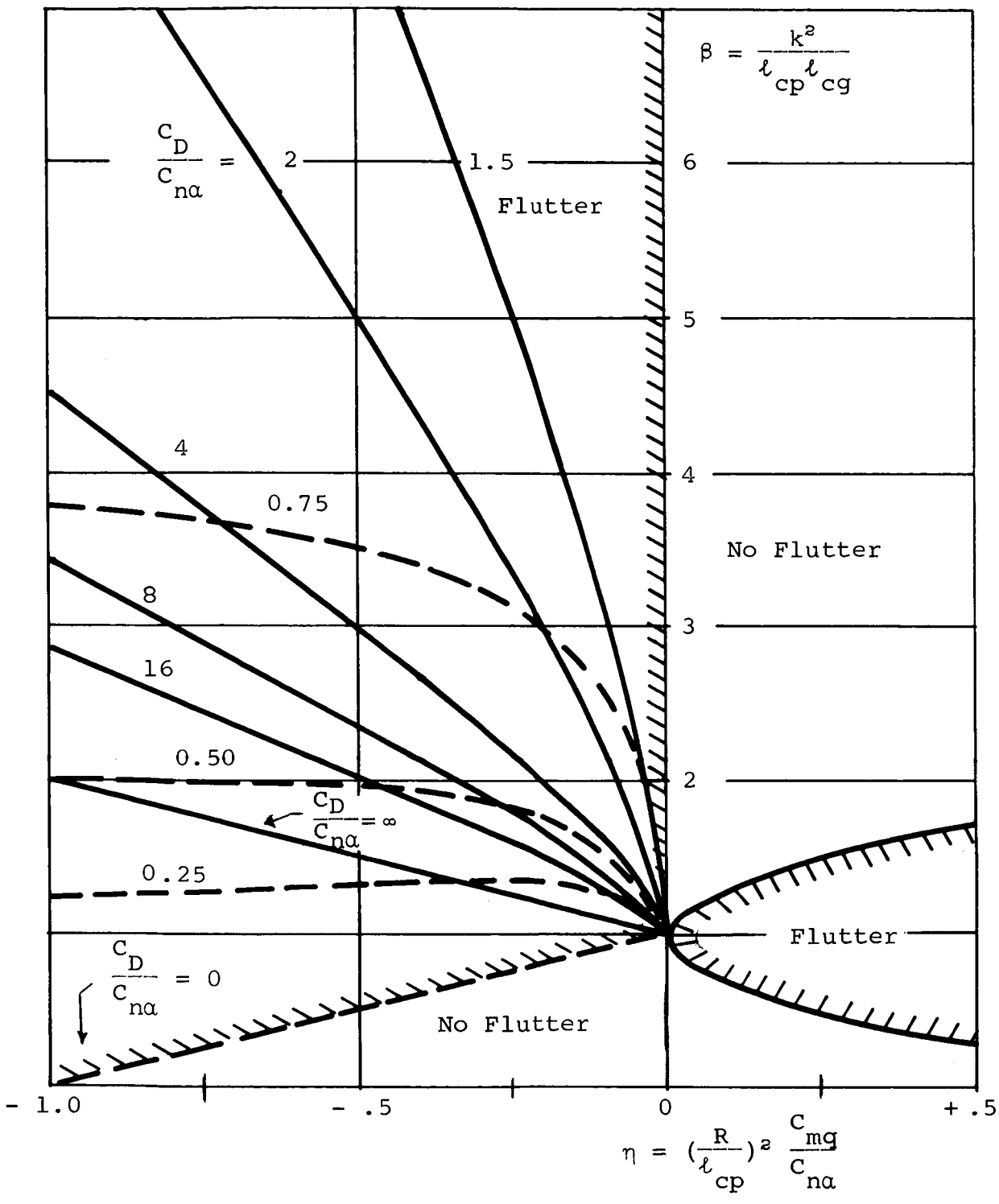

Figure 3 — Boundaries For Unconditional Stability of a Towed Drag Body, $C_{nq} = 0$.

$$\beta = \frac{k^2}{\ell_{cg}\ell_{cp}}$$ obtained from Figure 3

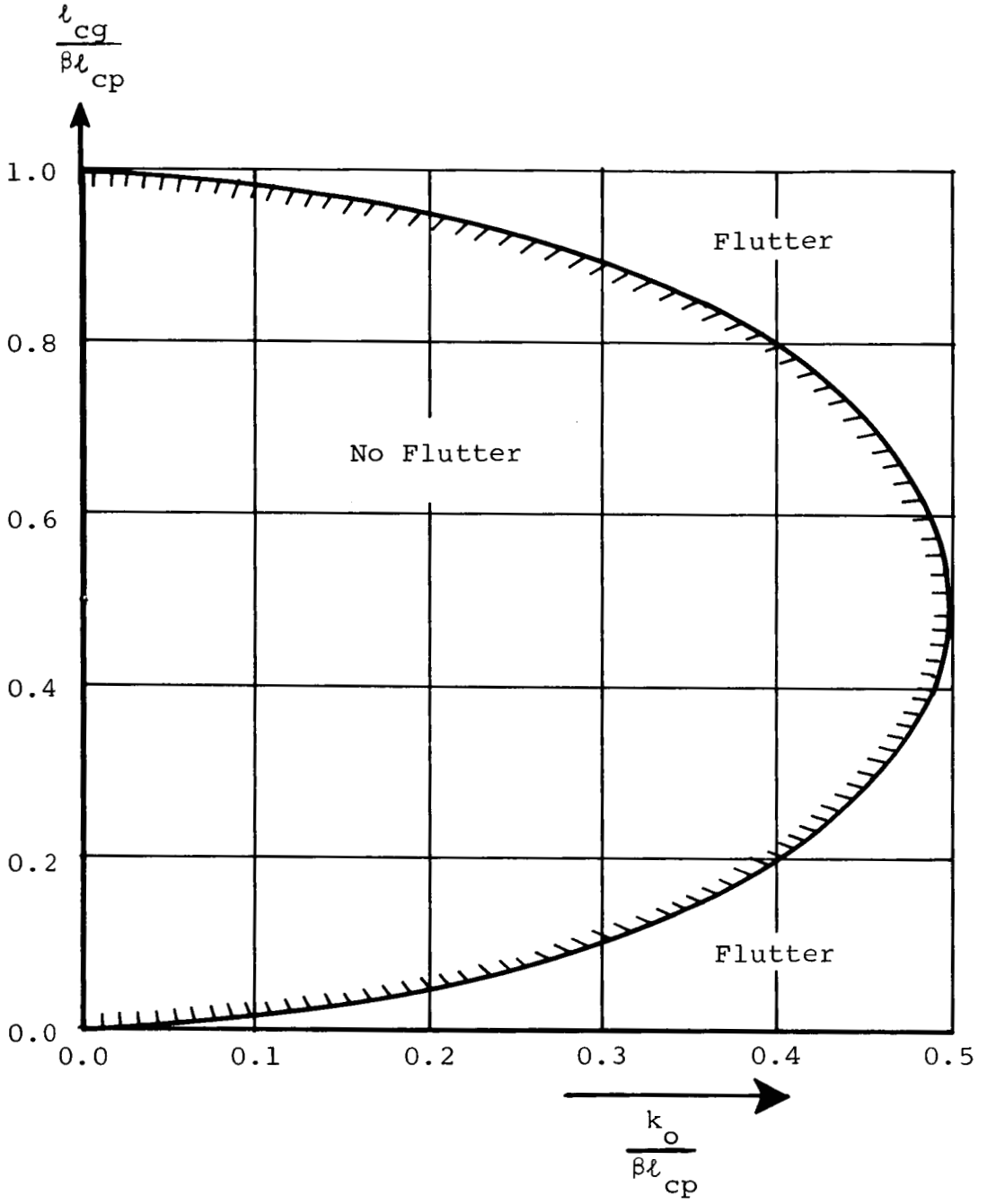

Figure 4 — Permissible Center of Gravity Range for Unconditional Stability

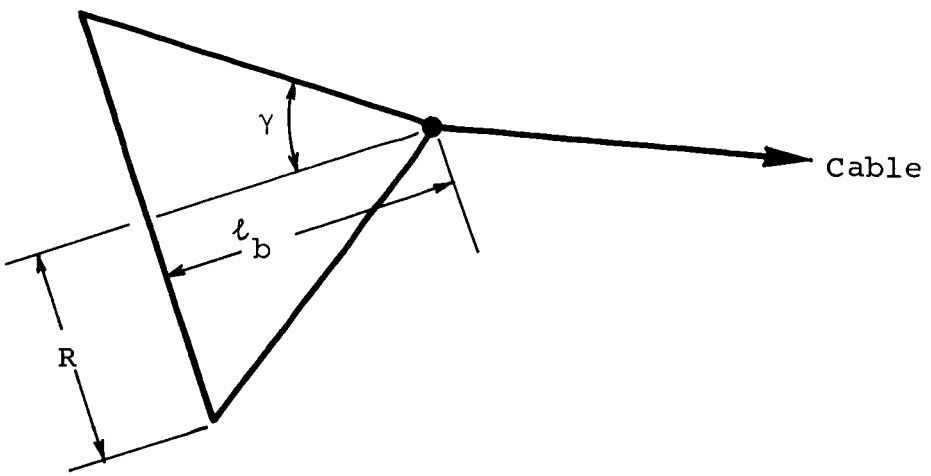

Figure 5 — Conical Decelerator

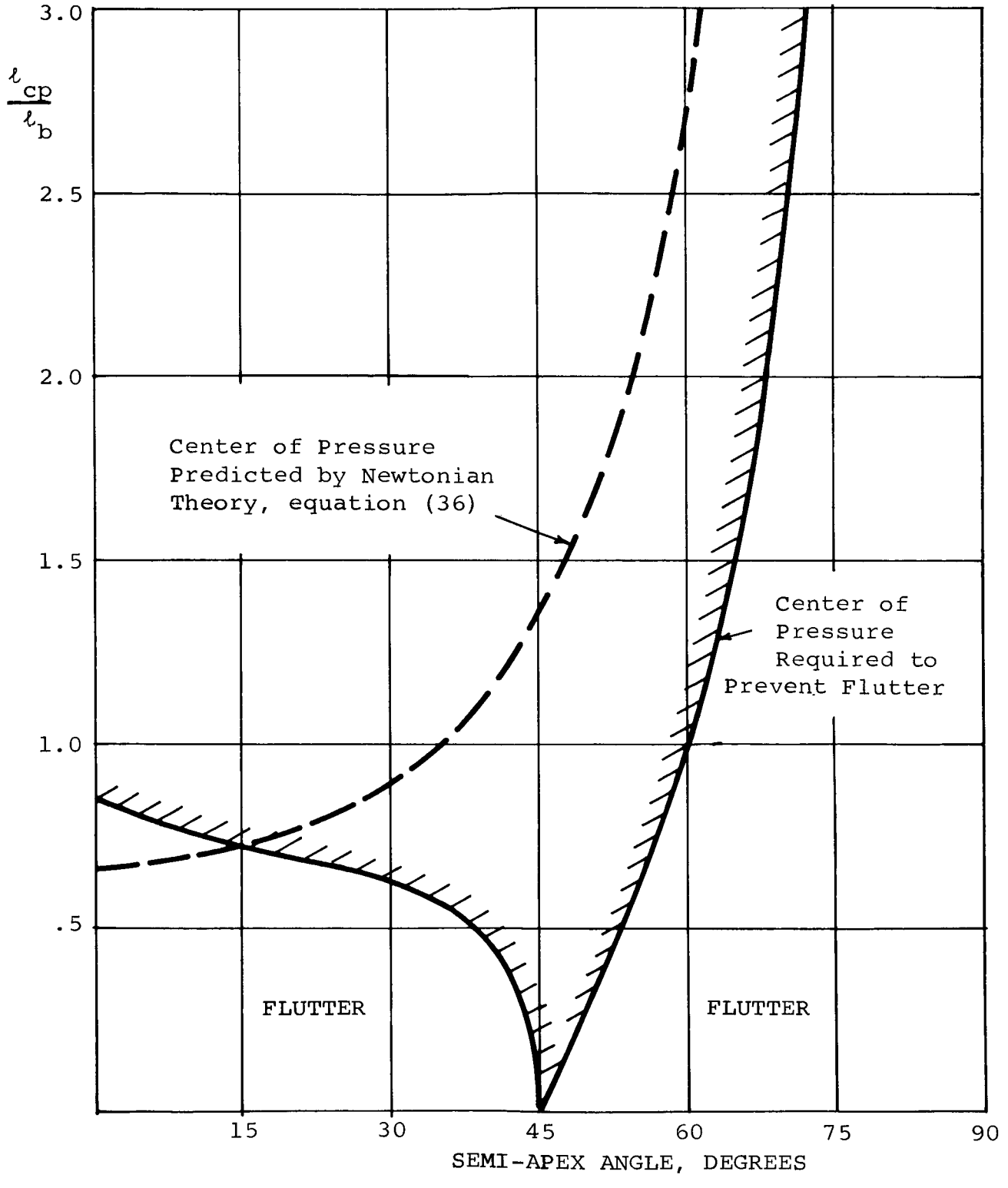

Figure 6 — Boundary For Unconditional Stability of a Uniform Conical Shell

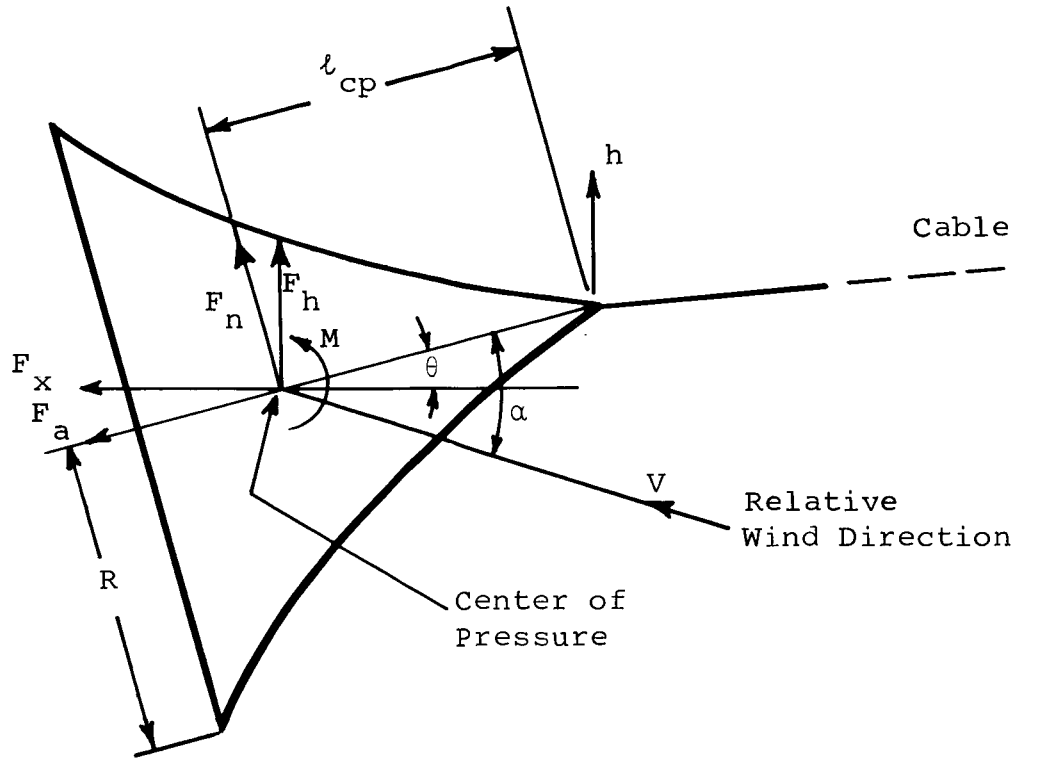

Figure B-1 — Aerodynamic Forces on Drag Body

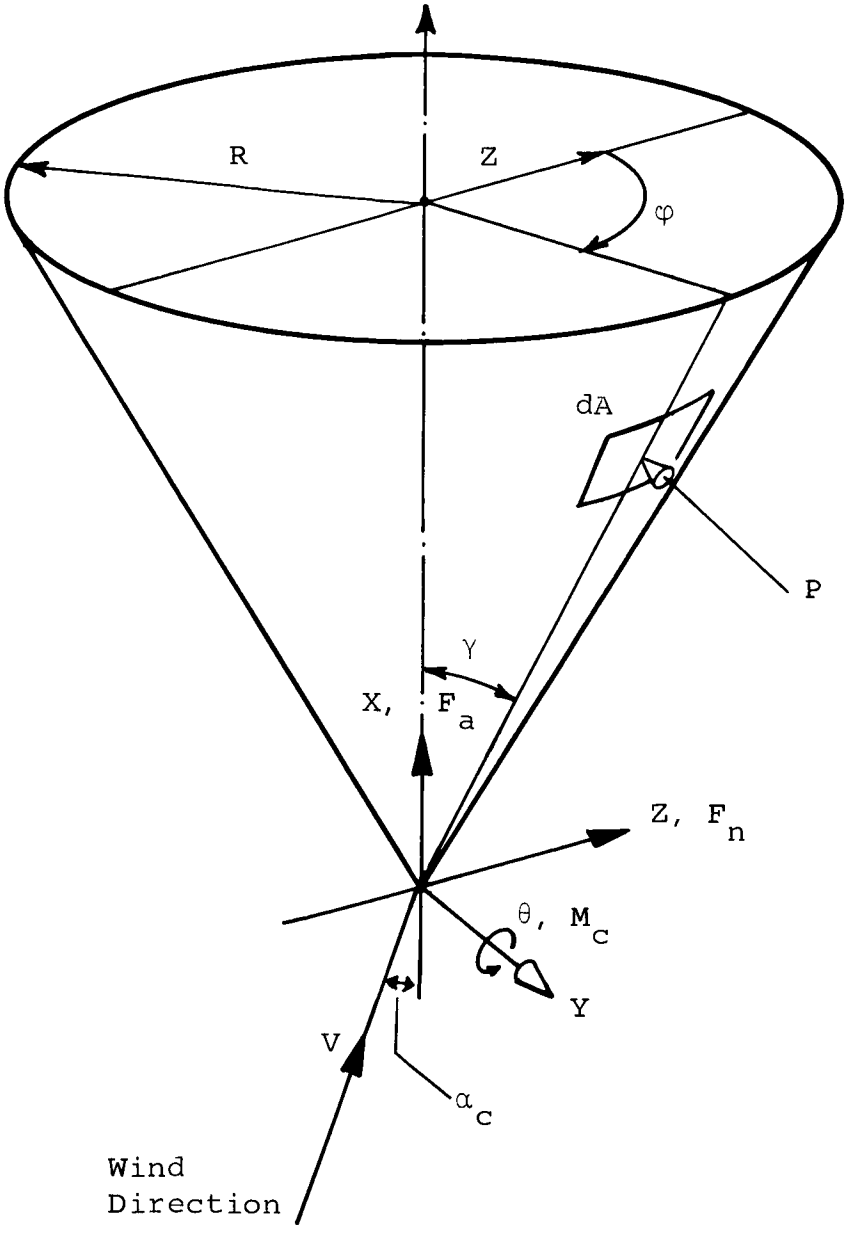

Figure C-1 — Aerodynamic Forces on a Cone

NASA-Langley, 1967 — 32 CR-766